

Concomitant antiferromagnetic transition and disorder-induced weak localization in an interacting electron system

Tanmoy Ghosh,¹ Takashi Fukuda,² Tomoyuki Kakeshita,² S. N. Kaul,³ and P. K. Mukhopadhyay^{1,*}

¹Laboratory for Condensed Matter Physics, Department of Condensed Matter Physics and Material Sciences, S. N. Bose National Centre for Basic Sciences, JD block, Sec-III, Salt Lake, Kolkata 700 106, India

²Department of Materials Science and Engineering, Graduate School of Engineering, Osaka University, 2-1, Yamada-oka Suita, Osaka 565-0871, Japan

³School of Physics, University of Hyderabad, Central University P.O., Hyderabad 500 046, Telangana, India

(Received 21 December 2016; revised manuscript received 14 March 2017; published 3 April 2017)

In this Rapid Communication we report a phenomenon in a disordered interacting electron system. The measurements of structural, magnetic, and transport properties of $\text{FeAl}_{2-x}\text{Ga}_x$ ($0 \leq x \leq 0.5$) show that antiferromagnetic transition in these intermetallic compounds occurs concomitantly with a disorder-induced weak localization of electrons; the temperatures T_N and T_m , at which antiferromagnetic transition and the weak localization respectively occur, closely track each other as the Ga concentration is varied. The antiferromagnetic transition is confirmed from the magnetic and specific heat measurements, and the occurrence of weak localization is confirmed from the temperature variation of resistivity and magnetoresistance measurements. With increasing Ga concentration, substitutional disorder in the system increases, and the consequent disorder-enhanced magnetic exchange interaction and disorder-induced fluctuations simultaneously drive antiferromagnetic transition and weak localization, respectively, to higher temperatures.

DOI: [10.1103/PhysRevB.95.140401](https://doi.org/10.1103/PhysRevB.95.140401)

Introduction. Both disorder [1,2] and electron-electron (e-e) interactions [3,4] cause metal-insulator transitions (MITs), although their basic mechanisms and properties of the insulating phases are distinctly different. Electron correlation-induced Mott MITs are characterized by an energy gap for charge-carrier excitations, whereas disorder-induced Anderson MITs have a singular relaxation time without any gap in their electronic density of states. When these effects coexist, which is often the case in condensed-matter systems, the interplay between them results in the emergence of novel phenomena [2,5–8]. In their coexistence, disorder and e-e interaction effects are largely seen as competitive where one obstructs the other [9–12]. MIT in two-dimensional systems is the quintessence of such competitive picture where e-e interactions disrupt the insulating state of the disordered system [7,13].

This impression of competitiveness extends to the magnetic ordering phenomena also where disorder-induced fluctuations are seen as a disruptive force [11,14–17]. Repulsive Coulomb interactions, due to electron correlations, cause single occupancy of electrons which favors magnetic ordering. On the other hand, electrons doubly occupy the lowest energy states to minimize the effect of disorder-induced fluctuations, thereby quenching the local moments and magnetic ordering.

Theoretical and numerical investigations [8,11,14–17] of the interplay between disorder and e-e interactions reveal that disorder destroys the insulating antiferromagnetic state originating from electron correlation in its weak limit, leading to a metallic paramagnetic phase. A metallic antiferromagnetic phase is also anticipated in the intermediate parameters regime. However, in the regime where both are strong, our understanding is severely limited due to the inherent difficulty of simultaneously incorporating them within a unified theoretical

framework. This situation is further compounded by the fact that controlled tuning of both e-e interactions and disorder is difficult in condensed-matter systems due to the disorder-induced fluctuations which tend to destabilize the underlying crystal structure of the system. General perception is that the naive picture of their competitiveness should break down in the strong disorder–strong e-e interaction regime leading to the emergence of novel phenomena. We present here a remarkable observation that antiferromagnetic transition temperature (T_N) in $\text{FeAl}_{2-x}\text{Ga}_x$ ($0 \leq x \leq 0.5$) increases with disorder and is accompanied by a resistivity minimum originating from disorder-induced enhanced e-e interaction and weak localization. We found that T_N and the temperature at which resistivity minimum appears, T_m , closely track each other as the Ga concentration is varied. This intriguing experimental finding raises questions on the widely accepted competitive picture [9–12,14–17] of disorder and electron correlations.

Crystal structure. FeAl_2 crystallizes into a triclinic structure (space group No. 2 and Pearson symbol $aP19$) comprising 19 atoms in the unit cell [18]. Figure 1(a) shows the arrangement of atoms in the unit cell. All the crystallographic sites are fully occupied by either Fe or Al atoms except for a single Wyckoff site of multiplicity 2 which could be occupied by either of the two atoms. This mixed occupancy of Fe and Al atoms causes substitutional disorder. Gallium addition results in a preferential occupation of the Al sites by Ga atoms (see Table S1, Table S2, and Fig. S1 in the Supplemental Material for the Rietveld refinement results [20]). This preference for the Al sites, combined with the mixed occupancy of Fe and Al atoms in the host, leads to increased disorder in the system with Ga substitution. The volume of the unit cell increased with increasing Ga concentration, as shown in Fig. 1(b).

Magnetic properties. FeAl_2 undergoes a spin-glass transition at $T_{sg} \approx 12$ K [21], and its magnetic properties could be described by a partially localized magnetic moment of Fe atoms [22]. Above T_{sg} , another magnetic transition appears

*Corresponding author: pkm@bose.res.in

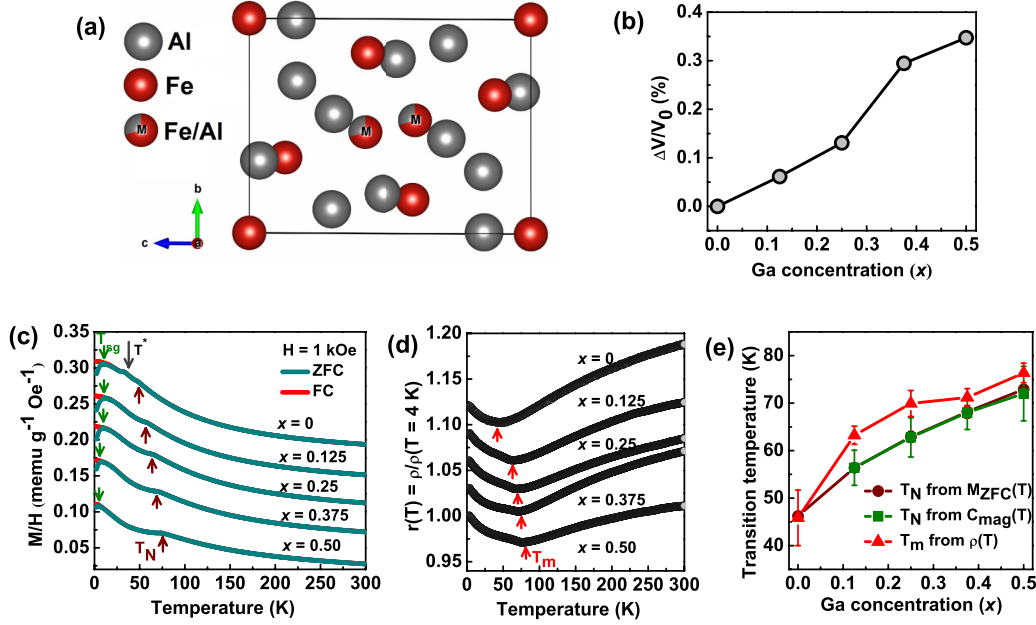


FIG. 1. (a) Arrangement of Fe and Al atoms in the unit cell of FeAl_2 . VESTA (Ref. [19]) is used to draw the unit-cell representation. (b) Change in unit-cell volume as a function of Ga concentration in $\text{FeAl}_{2-x}\text{Ga}_x$ ($0 \leq x \leq 0.5$). Crystal structure parameters obtained from Rietveld refinement are given in the Supplemental Material [20]. (c) Temperature dependence of ZFC and FC magnetizations of $\text{FeAl}_{2-x}\text{Ga}_x$. Upward (wine) and downward (olive) vertical arrows indicate the antiferromagnetic transition temperature T_N and spin-glass transition temperature T_{sg} , respectively. Downward gray arrow indicates the second magnetic transition at T^* observed only in the composition $x = 0$. (d) Temperature dependence of resistivity in $\text{FeAl}_{2-x}\text{Ga}_x$. Upward red arrows indicate the position of resistivity minimum. (e) Variation with Ga composition of the antiferromagnetic transition temperature (T_N) and the temperature at which the resistivity minimum occurs (T_m). Graphs in (c) and (d) are successively shifted upward from $x = 0.50$ composition data by 0.04 and 0.03, respectively, on the Y scale for clarity.

whose nature is highly controversial [21–24]. The temperature variations of “zero-field-cooled” (ZFC) and “field-cooled” (FC) magnetizations of $\text{FeAl}_{2-x}\text{Ga}_x$ are shown in Fig. 1(c). The bifurcation between ZFC and FC magnetizations at low temperatures (see Fig. S2 in the Supplemental Material for an enlarged view [20]), present in all the compositions, indicates that the spin-glass behavior of FeAl_2 persists up to the highest Ga composition. While the spin-glass behavior of FeAl_2 was studied extensively, the effect of Ga addition on the spin-glass state has not been investigated before and could form a subject for another investigation. In this work, we are interested in the magnetic transition at T_N ($T_N > T_{sg}$) which manifests itself as a broad hump in $x = 0$ and gradually evolves into a prominent peak, which shifts to higher temperatures with increasing Ga concentration. We fitted the $M_{ZFC}(T)$ (see Fig. S3 in the Supplemental Material [20]), in the paramagnetic region, with Curie-Weiss law $\chi = \chi_0 + \frac{C}{T-\theta}$, where χ_0 is the temperature-independent part of the susceptibility, C is the Curie-Weiss constant, and θ is the temperature characterizing spin-spin interactions. θ is found to be *negative* in all the compositions (listed in Table I), suggesting the antiferromagnetic nature of the spin interactions. ZFC and FC magnetizations do not show any signature of irreversibility on passing through T_N . Consistent with the antiferromagnetic nature of magnetic ordering, the magnetization-field (M - H) isotherms, taken below T_N [shown in Fig. 2(a)], are linear up to the highest magnetic field of 50 kOe. As shown in the inset of Fig. 2(a), no hysteresis in the M - H curves is observed, suggesting the absence of any ferromagnetic

couplings or isolated spin impurities in this temperature range. Earlier studies of magnetization, Mössbauer, and neutron diffraction also suggested the antiferromagnetic nature of this transition at T_N in FeAl_2 , however, the values of T_N did not agree [21,24]. Our magnetization measurements indicate two magnetic transitions above T_{sg} at T_N and T^* ($T_N > T^* > T_{sg}$), and we contend that previous studies detected either of these transitions (i.e., at T^* or T_N), resulting in the disagreement in the reported transition temperatures.

Specific heat. The magnetic part of the specific heat (C_{mag}) for different compositions is shown in Figs. 2(b)–2(e). Although our method of calculation does not allow us to extract C_{mag} for the composition $x = 0$ or to determine the absolute value of C_{mag} accurately, peaks corresponding to the magnetic transitions are clearly discernible in these graphs. Variation of T_N with Ga concentration, obtained from the peak position in

TABLE I. Values of the temperature-independent part of the susceptibility χ_0 , Curie-Weiss temperature θ , and magnetic moment of Fe, μ_{Fe} , obtained from fitting the paramagnetic region of ZFC magnetization curves of $\text{FeAl}_{2-x}\text{Ga}_x$ with Curie-Weiss law.

x	χ_0 (emu g ⁻¹ Oe ⁻¹)	θ (K)	μ_{Fe} (μ_B)
0	6.7×10^{-6}	-20.1	2.76
0.125	2.5×10^{-6}	-30.2	2.96
0.25	2.1×10^{-6}	-31.3	3.10
0.375	1.8×10^{-6}	-45.0	3.24
0.50	5.6×10^{-7}	-57.5	3.18

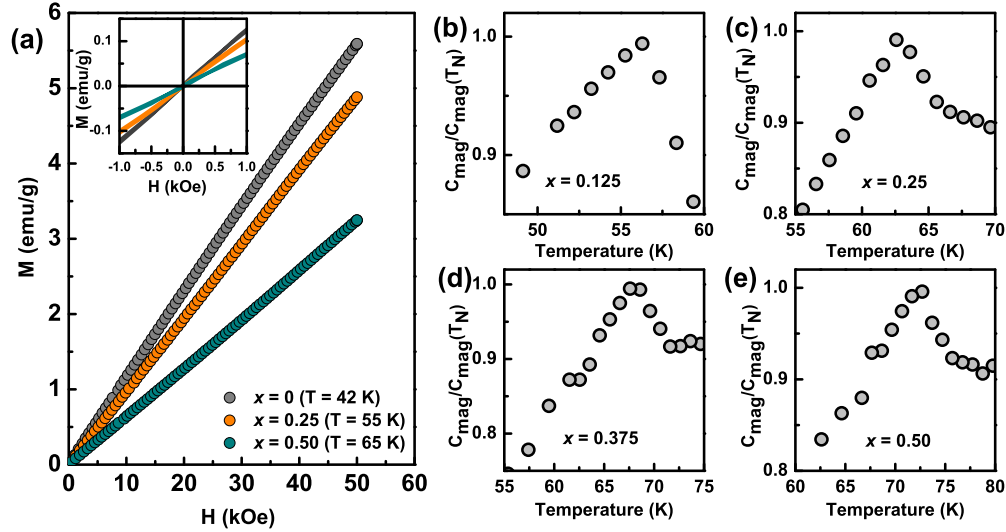


FIG. 2. (a) Magnetization-field (M - H) isotherms for $\text{FeAl}_{2-x}\text{Ga}_x$ measured below T_N . Inset depicts the enlarged view of the M - H isotherms near the origin. (b)–(e) highlight the peak in the magnetic part of the specific heat, C_{mag} , of $\text{FeAl}_{2-x}\text{Ga}_x$ in the vicinity of the antiferromagnetic transition. Details of the extraction of C_{mag} from total specific heat C_p are given in the Supplemental Material [20].

$C_{\text{mag}}(T)$, is shown in Fig. 1(e) which highlights an excellent agreement with T_N obtained from the magnetization data.

Resistivity. Electrical resistivity (ρ) as a function of temperature exhibits minima [Fig. 1(d)] in all the compositions. The most striking observation is that T_m closely follows T_N , as is evident from Fig. 1(e), when the Ga concentration varies. Resistivity minimum in disordered solids results from two competing mechanisms. The disorder-aided enhancement in the electron-electron interactions (EEIs), due to diffusive electron motion, and weak localization (WL) of electrons, by the quantum interference effect, lead to the increase in resistivity as the temperature is lowered below T_m [5] whereas the inelastic-scattering processes progressively destroy the phase coherence so as to restore the classical Boltzmann (ballistic) transport behavior for $T > T_m$. In three-dimensional (3D) systems at very low temperatures, the contribution to

resistivity from the EEI effects ($\rho_{\text{EEI}} \sim \sqrt{T}$) dominates over that due to WL effects [5] ($\rho_{\text{WL}} \sim T^{p/2}$, where the value of the index p depends on the type of inelastic-scattering process that dominates in a given temperature range). Figure 3(a) clearly bears out that the EEI effects dominate $\rho(T)$ up to ~ 20 K in $\text{FeAl}_{2-x}\text{Ga}_x$. In pure (ordered) metals, $\rho(T)$ has contributions from inelastic scattering of electrons by phonons ($\rho_{\text{e-ph}}$) and electrons ($\rho_{\text{e-e}}$) such that $\rho_{\text{e-e}}(T)$ dominates over $\rho_{\text{e-ph}}(T)$ at very low temperatures, while the reverse is true at intermediate and high temperatures. In the Fe-Al system, electron correlation effects become increasingly important with increasing Al concentration as is evidenced by enhanced electronic specific heat in the Al-rich compound Fe_2Al_5 [25] and the crucial role it plays in determining the magnetic ground state of the equiatomic compound FeAl [26,27]. Consistent with these reports, the value of the electronic specific heat

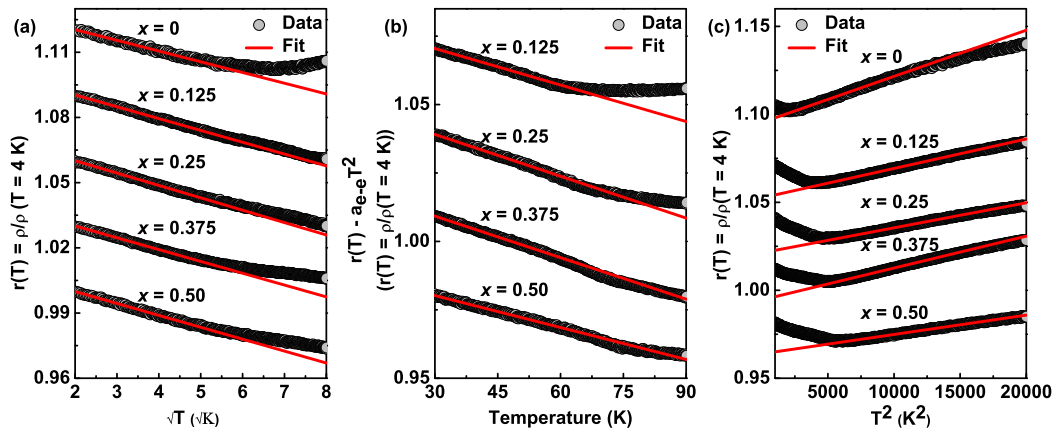


FIG. 3. (a) Linear relationship between resistivity and \sqrt{T} at low temperatures establishes the dominance of disorder-enhanced EEIs at such temperatures in $\text{FeAl}_{2-x}\text{Ga}_x$. (b) Fit to the resistivity data of $\text{FeAl}_{2-x}\text{Ga}_x$ at temperatures below the resistivity minimum (i.e., at $T < T_m$) considering both the inelastic electron-electron scattering ($\rho_{\text{e-e}}$) and weak localization (ρ_{WL}) contributions to resistivity. The temperature range below the resistivity minimum but above the EEI-dominated region is very small particularly in the composition $x = 0$. This precludes such a fit with reliable fitting parameters for $x = 0$. (c) T^2 dependence of resistivity in $\text{FeAl}_{2-x}\text{Ga}_x$ above the minimum originating from the inelastic electron-phonon scattering. Graphs in (a)–(c) are successively shifted upward from $x = 0.50$ composition data by 0.03 on the Y scale for clarity.

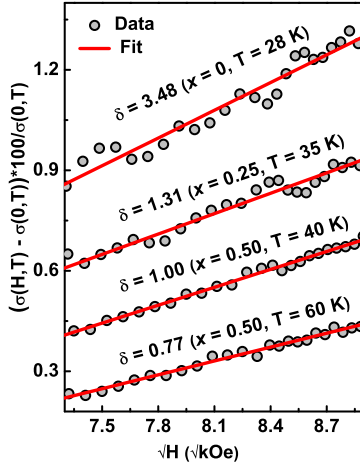


FIG. 4. Linear dependence of $\Delta\sigma$ on \sqrt{H} due to the disorder-induced weak localization in $\text{FeAl}_{2-x}\text{Ga}_x$. Graphs are successively shifted upward from $x = 0.50$ at $T = 60$ K by 0.15 on the Y scale for clarity.

coefficient in $\text{FeAl}_{2-x}\text{Ga}_x$ is approximately $25 \text{ mJ mol}^{-1} \text{K}^{-2}$ (see Table S3 in the Supplemental Material [20]); typical of $3d$ heavy-fermion-like systems. Thus, in the temperature range which lies above the EEI-dominated region but below T_m , dominant contributions to resistivity are expected to come from $\rho_{e-e}(T) \sim T^2$ and ρ_{WL} (with the index $p = 2$ in the expression for ρ_{WL} [5]). Figure 3(b) validates this expectation. In disordered metallic systems, at intermediate temperatures, the inelastic electron-phonon scattering contribution to $\rho(T)$, $\rho_{e-ph}(T)$ (also varying with temperature as T^2 [28,29]) is so large as to swamp $\rho_{e-e}(T)$. T^2 variation of resistivity, observed in $\text{FeAl}_{2-x}\text{Ga}_x$ at temperatures above the resistivity minimum [shown in Fig. 3(c)] thus reflects a dominant $\rho_{e-ph}(T)$.

Magnetoresistance. One of the decisive ways to identify WL is to study magnetoresistance (MR), which has unique characteristic behavior for weakly localized systems. WL theory predicts that MR is *negative* in 3D systems and at high magnetic field change in conductivity, $\Delta\sigma(H, T) = \sigma(H, T) - \sigma(0, T)$, is proportional to \sqrt{H} with a slope $\delta = 0.918$ when H and σ are respectively expressed in units of kOe and $\Omega^{-1} \text{cm}^{-1}$ [30,31]. $\Delta\sigma(H, T)$ due to the EEI effects also varies with field as \sqrt{H} , however, the MR in that case is *positive* [5]. Since ρ_{EEI} almost entirely accounts for the resistivity of $\text{FeAl}_{2-x}\text{Ga}_x$ below 20 K, MR was measured above 20 K to avoid appreciable contribution from the EEI effects. The linear

variation of $\Delta\sigma$ with \sqrt{H} displayed in Fig. 4 clearly validates the WL scenario. The values of δ obtained for $x = 0.25$ and 0.50 (Fig. 4) agree well with that predicted by the WL theory [30,31]. Large deviation of δ from theoretical prediction in the composition $x = 0$ might be related to the presence of another magnetic transition at $T^* \approx 32$ K.

Discussion. The above experimental observations are notable on several counts. The increase in T_N with disorder—a scenario for strong electron correlation limit—is anticipated for a long time [16,32,33]. The expectation is that increasing disorder results in the enhancement of magnetic exchange interactions [16,32,33] which subsequently increases T_N . This disorder-aided enhancement of exchange interaction in $\text{FeAl}_{2-x}\text{Ga}_x$ is clearly evident from the increase in $|\theta|$ (listed in Table I) with Ga concentration, i.e., disorder. However, the occurrence of antiferromagnetic transition simultaneous with weak localization (i.e., $T_N \approx T_m$) is more astonishing. The partially localized magnetic moment of Fe atoms [22] and T^2 dependence of resistivity, observed at lower temperatures, are reminiscent of the two-fluid behavior [8,34,35] of the system comprising itinerant quasiparticles and local moments. In the two-fluid picture, a local moment forms at a site if the site energy $|\varepsilon_i| < U/2$ (U is the on-site Coulomb repulsion), whereas the electrons on the sites with energy $|\varepsilon_i| > U/2$ are itinerant and experience localization at temperatures below T_m [12,15,36]. These local moments are weakly coupled to the conduction electron cloud and interact with one another via Ruderman-Kittel-Kasuya-Yosida interaction. Disorder-induced spatial fluctuations cause an inhomogeneous distribution of these moments. Such an inhomogeneous distribution of local moments is expected to have a low-temperature spin-glass ground state [8,37]. Indeed, as the phase-coherence length progressively increases with lowering of temperature, the antiferromagnetic state of $\text{FeAl}_{2-x}\text{Ga}_x$ gives way to the spin-glass state.

Conclusion. The disorder-enhanced magnetic exchange interaction and disorder-induced fluctuations simultaneously drive T_N and T_m , respectively, to higher temperatures with increasing disorder. While the disorder-aided enhancement of T_N is anticipated before, the observation $T_N \approx T_m$ is notable. This observed concomitant nature of T_N and T_m in $\text{FeAl}_{2-x}\text{Ga}_x$ underscores the need to revisit the theoretical frameworks that deal with the interplay between disorder and electron-electron interactions.

Acknowledgment. T.G. and P.K.M. thank Prof. A. K. Raychaudhuri of S. N. Bose National Centre for Basic Sciences, Kolkata, India, for extending use of the magnetoresistance measurement facility.

[1] P. W. Anderson, *Phys. Rev.* **109**, 1492 (1958).
 [2] *50 Years of Anderson Localization*, edited by E. Abrahams (World Scientific, Singapore, 2010).
 [3] N. F. Mott, *Proc. Phys. Soc., London, Sect. A* **62**, 416 (1949).
 [4] N. F. Mott, *Rev. Mod. Phys.* **40**, 677 (1968).
 [5] P. A. Lee and T. V. Ramakrishnan, *Rev. Mod. Phys.* **57**, 287 (1985).
 [6] D. Belitz and T. R. Kirkpatrick, *Rev. Mod. Phys.* **66**, 261 (1994).

[7] B. Spivak, S. V. Kravchenko, S. A. Kivelson, and X. P. A. Gao, *Rev. Mod. Phys.* **82**, 1743 (2010).
 [8] E. Miranda and V. Dobrosavljević, *Rep. Prog. Phys.* **68**, 2337 (2005).
 [9] L. Sanchez-Palencia, *Nat. Phys.* **6**, 328 (2010).
 [10] K. Byczuk, W. Hofstetter, and D. Vollhardt, *Phys. Rev. Lett.* **94**, 056404 (2005).
 [11] K. Byczuk, W. Hofstetter, and D. Vollhardt, *Phys. Rev. Lett.* **102**, 146403 (2009).

- [12] M. C. O. Aguiar, V. Dobrosavljević, E. Abrahams, and G. Kotliar, *Phys. Rev. Lett.* **102**, 156402 (2009).
- [13] A. Punnoose and A. M. Finkel'stein, *Science* **310**, 289 (2005).
- [14] D. Heidarian and N. Trivedi, *Phys. Rev. Lett.* **93**, 126401 (2004).
- [15] M. A. Tusch and D. E. Logan, *Phys. Rev. B* **48**, 14843 (1993).
- [16] M. Ulmke, V. Janiš, and D. Vollhardt, *Phys. Rev. B* **51**, 10411 (1995).
- [17] H. Shinaoka and M. Imada, *Phys. Rev. Lett.* **102**, 016404 (2009).
- [18] I. Chumak, K. W. Richter, and H. Ehrenberg, *Acta Crystallogr., Sect. C: Cryst. Struct. Commun.* **66**, i87 (2010).
- [19] K. Momma and F. Izumi, *J. Appl. Crystallogr.* **44**, 1272 (2011).
- [20] See Supplemental Material at <http://link.aps.org/supplemental/10.1103/PhysRevB.95.140401> for experimental methods, XRD patterns and crystal structure parameters, enlarged view of ZFC-FC magnetization curves at low temperature, fittings of temperature variation of ZFC magnetizations with Curie-Weiss law, and analysis of specific heat and resistivity data.
- [21] Z. Jagličić, S. Vrtnik, M. Feuerbacher, and J. Dolinšek, *Phys. Rev. B* **83**, 224427 (2011).
- [22] J. Chi, Y. Li, F. G. Vagizov, V. Goruganti, and J. H. Ross, Jr., *Phys. Rev. B* **71**, 024431 (2005).
- [23] C. S. Lue, Y. Öner, D. G. Naugle, and J. H. Ross, Jr., *Phys. Rev. B* **63**, 184405 (2001).
- [24] D. Kaptás, E. Sváb, Z. Somogyvári, G. André, L. F. Kiss, J. Balogh, L. Bujdosó, T. Kemény, and I. Vincze, *Phys. Rev. B* **73**, 012401 (2006).
- [25] J. Chi, X. Zheng, S. Y. Rodriguez, Y. Li, W. Gou, V. Goruganti, K. D. D. Rathnayaka, and J. H. Ross, *Phys. Rev. B* **82**, 174419 (2010).
- [26] P. Mohn, C. Persson, P. Blaha, K. Schwarz, P. Novák, and H. Eschrig, *Phys. Rev. Lett.* **87**, 196401 (2001).
- [27] A. Galler, C. Taranto, M. Wallerberger, M. Kaltak, G. Kresse, G. Sangiovanni, A. Toschi, and K. Held, *Phys. Rev. B* **92**, 205132 (2015).
- [28] P. D. Babu, S. N. Kaul, L. F. Barquín, J. C. G. Sal, W. H. Kettler, and M. Rosenberg, *Int. J. Mod. Phys. B* **13**, 141 (1999).
- [29] S. Srinivas, S. N. Kaul, and S. N. Kane, *J. Non-Cryst. Solids* **248**, 211 (1999).
- [30] A. Kawabata, *Solid State Commun.* **34**, 431 (1980).
- [31] A. Kawabata, *J. Phys. Soc. Jpn.* **49**, 628 (1980).
- [32] Y. H. Szczech, M. A. Tusch, and D. E. Logan, *J. Phys.: Condens. Matter* **10**, 639 (1998).
- [33] A. Singh, M. Ulmke, and D. Vollhardt, *Phys. Rev. B* **58**, 8683 (1998).
- [34] M. A. Paalanen, J. E. Graebner, R. N. Bhatt, and S. Sachdev, *Phys. Rev. Lett.* **61**, 597 (1988).
- [35] R. N. Bhatt and D. S. Fisher, *Phys. Rev. Lett.* **68**, 3072 (1992).
- [36] M. C. O. Aguiar, V. Dobrosavljević, E. Abrahams, and G. Kotliar, *Phys. Rev. B* **73**, 115117 (2006).
- [37] S. Sachdev, *Philos. Trans. R. Soc., A* **356**, 173 (1998).